DGFMIL: Fuzzy Multi-Instance Learning with Cross-Granularity Calibration and Soft Semantic Routing for Histopathological Image Staging

Meiling Cai[1][0009−0000−8690−4067], Juanjuan Zhao[1,2⋆][0000−0001−8134−9076], Wensong Yue[1][0009−0004−0776−6129], Lin Zhao[3][0009−0002−9037−4227], Yue Zeng[1][0009−0006−6638−4168], Lijing Zhang[1][0000−0002−7190−0829], and Yan Qiang[4][0000−0001−6231−3721]

[1] College of Computer Science and Technology (College of Data Science), Taiyuan University of Technology, Taiyuan, China
[2] School of Software, Taiyuan University of Technology, Taiyuan, China
zhaojuanjuan@tyut.edu.cn
[3] School of Computer Science and Engineering, Southeast University, Nanjing, China
[4] School of Software, North University of China, Taiyuan, China

Abstract. Pathological staging is critical for cancer diagnosis and treatment. However, extracting interpretable features from high-resolution whole slide images (WSIs) for accurate staging remains challenging. Existing methods divide WSIs into numerous patches but face two fundamental issues: lack of fine-grained stage labels and mixed-stage morphology within a single patch. Simply assigning a single pseudo-label discards heterogeneity and leads to decisions lacking medical interpretability. To address this, we propose DGFMIL, a dual-granularity fuzzy multiple instance learning framework centered on uncertainty modeling and semantic prior alignment. First, we introduce a differentiable interval type-2 fuzzification function that explicitly assigns a possibility interval rather than a single stage label to capture intrinsic heterogeneous staging characteristics. Second, cross-granularity calibration and fuzzy-guided cross-attention serve as auxiliary mechanisms to refine the representation and fusion of fuzzy features. Third, we construct a pathological concept text bank and impose semantic prior constraints on each patch via a routing soft alignment, enforcing visual representations to align with interpretable medical concepts. Extensive experiments on TCGA-CRC and Camelyon17 datasets demonstrate that DGFMIL achieves strong competitive performance.

Keywords: Computational pathology · Multiple instance learning · Uncertainty quantification · Fuzzy logic.

1 Introduction

Automated staging of whole slide images (WSIs) in histopathology [14, 22] is critical for cancer diagnosis, treatment planning, and prognosis assessment [3,

⋆ Corresponding author.

17]. In recent years, multiple instance learning (MIL) has emerged as the dominant paradigm for processing gigapixel-scale WSIs [12], achieving significant progress in cancer subtype classification [4] and survival prediction [26]. However, existing MIL methods face a fundamental representation dilemma in practical deployment: when a WSI is divided into thousands of unlabeled patches, the staging status of each patch is inherently ambiguous and heterogeneous—the same patch may exhibit pathological features that coexist across multiple stages, while adjacent patches may have markedly different stage labels [1, 8]. This intrinsic patch-level uncertainty, intertwined with the continuous nature of the staging process, makes it challenging for traditional hard-assignment MIL to achieve reliable modeling.

The challenges in existing approaches manifest in three aspects. First, pathological staging is a continuous and gradual process, where the morphological characteristics of boundary cases exhibit ambiguous transitions [7]. Traditional deep learning models, which rely on deterministic predictions, are prone to overconfident misclassifications at these boundaries [10] and lack the capability to quantify the plausible staging range for an individual patch. More critically, existing MIL methods treat a WSI as a bag of instances, implicitly assuming that all patches share the same latent label. This simplifying assumption completely overlooks the staging heterogeneity at the patch level—a stark contradiction to the reality observed by pathologists under the microscope, where regions of varying differentiation grades often coexist within a single high-power field [18, 23]. Third, there is a semantic gap between data-driven visual features and clinical diagnostic criteria [2, 5]. Pathologists reason based on textual descriptions in medical guidelines (e.g., marked nuclear atypia, disordered glandular architecture), whereas deep models optimize within an abstract feature space, lacking alignment with interpretable medical concepts [25, 16].

In response to the aforementioned challenges, this paper proposes the DGFMIL (Deep Granular Fuzzy Multiple Instance Learning) framework. Its core innovation lies in the first-ever integration of Interval Type-2 Fuzzy Set theory [19, 11] with Multiple Instance Learning, enabling instance-level uncertainty quantification and semantic constraints without requiring patch-level annotations. Unlike existing MIL methods that model uncertainty using probability distributions or evidential learning [27], DGFMIL introduces a differentiable Interval Type-2 fuzzification mechanism. It constructs membership intervals, rather than deterministic values, for each unlabeled patch. By leveraging the three-dimensional membership function of fuzzy sets, it explicitly captures the Footprint of Uncertainty (FOU) at staging boundaries, achieving a pioneering patch-level fuzzy uncertainty footprint tracking within the MIL framework. Different from existing text-guided methods that rely on paired data [9] or slide-level alignment [13], this paper constructs a medical text description library related to staging. Through a Routing Soft Alignment Module (RSAM), it achieves zero-shot fine-grained alignment between patch features and the clinical concepts of WHO grading, embedding interpretable medical priors under sparsity constraints. While outputting high-precision staging results, DGFMIL provides uncertainty estimates

and semantic explanations for each patch, significantly enhancing the model's decision-making reliability on borderline cases.

The main contributions of this work are summarized as follows:

1. Proposes the first Interval Type-2 Fuzzy Multiple Instance Learning framework. By introducing a differentiable Interval Type-2 fuzzification mechanism, it constructs membership intervals for unlabeled patches, enabling the explicit modeling of patch-level staging uncertainty.
2. Achieves zero-shot injection of medical priors. It constructs a staging-related medical text description library and employs a routing soft alignment to achieve fine-grained alignment between patch features and the clinical concepts of WHO grading.
3. Establishes a unified paradigm for uncertainty quantification and semantic interpretation. It simultaneously provides uncertainty estimates and medical semantic explanations for each patch, thereby enhancing decision-making reliability for borderline cases.

2 Methods

2.1 Overview

Fig. 1 depicts the pipeline of the proposed DGFMIL framework. Given a WSI, we first extract global thumbnail features and local patch features. The core innovation lies in two synergistic pathways: Path 1 is the uncertainty-aware path, which maps visual features into membership intervals with a footprint of uncertainty via Interval Type-2 fuzzification, and refines the fuzzy feature representation using cross-granularity information. Path 2 is the semantic prior path, which dynamically associates patch features with a pathological text concept library through routing soft alignment to inject interpretable medical priors. The outputs from both pathways are ultimately integrated to achieve cancer staging.

2.2 Uncertainty-Aware Path

This path aims to quantify patch-level staging uncertainty and refine the fuzzy feature representation using cross-granularity context.

Interval Type-2 Fuzzification with Cross-Granularity Refinement We map the input patch features $\mathbf{X}$ into K Interval Type-2 Fuzzy Sets (IT2FS), where each set represents a specific disease stage. Unlike Type-1 fuzzy sets, IT2FS introduces a Footprint of Uncertainty (FOU) bounded by an Upper Membership Function (UMF, $\overline{\mu}$) and a Lower Membership Function (LMF, $\underline{\mu}$). Utilizing Gaussian membership functions defined by mean $\mathbf{m}_k$, standard deviation

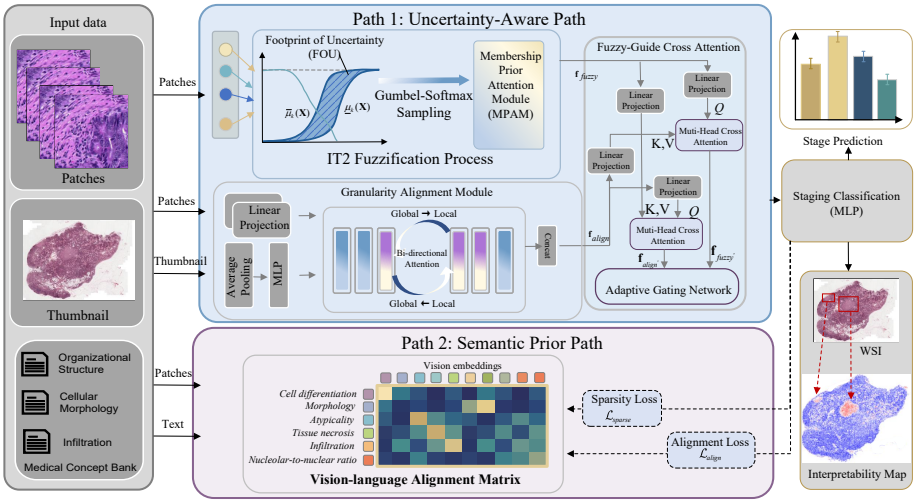

Fig. 1. Overall framework diagram of DFGMIL, which consists of two branches: Path 1 is the uncertainty-aware branch, and Path 2 is the semantic prior branch. The model ultimately achieves cancer staging.

σ_k, and uncertainty parameter δ_k, we define:

$$\underline{\mu}_k(\mathbf{X}) = \exp\left(-\frac{1}{2}\left(\frac{\mathbf{X}-(\mathbf{m}_k-\delta_k)}{\sigma_k}\right)^2\right), \overline{\mu}_k(\mathbf{X}) = \exp\left(-\frac{1}{2}\left(\frac{\mathbf{X}-(\mathbf{m}_k+\delta_k)}{\sigma_k}\right)^2\right), \tag{1}$$

This mapping yields a membership interval $[\underline{\mu}_k(\mathbf{x}), \overline{\mu}_k(\mathbf{x})]$, which explicitly captures the inherent range of possibilities when grading samples with ill-defined boundaries. To integrate the non-differentiable Karnik-Mendel algorithm into the neural network, we propose a reparameterization trick. We uniformly sample S points within the FOU and assign weights using the Gumbel-Softmax distribution. This allows for the computation of the reduced membership score μ_k^{reduced} and the uncertainty measure $U_k(\mathbf{X})$ (i.e., the interval width) while maintaining gradient flow.

Membership Prior Attention Mechanism (MPAM) To prevent overfitting in few-shot scenarios, we utilize μ_k^{reduced} as a strong prior. The attention weights A are computed by fusing a prior-based branch (derived directly from soft-normalized membership grades) and a data-driven branch (processed via a two-layer MLP), controlled by a learnable gating parameter λ . Crucially, we modulate the weights using the uncertainty measure to suppress high-uncertainty features:

$$\mathbf{A} = \left(\lambda \cdot \text{Softmax}(\mu^{\text{reduced}}) + (1-\lambda)\cdot \mathbf{A}_{\text{data}}\right) \odot (1-\beta U_k(\mathbf{X})) \tag{2}$$

The final output is a fuzzy feature representation $\mathbf{F}_{fuzzy}$ that encodes both discriminative patterns and their associated reliability.

Granularity Alignment Module (GAM) Pathological diagnosis relies on correlating macro-scale tissue architecture (thumbnails) with micro-scale cellular details (patches). The Global-to-Local Alignment Module (GAM) explicitly models this cross-scale interaction. Let $\mathbf{f}_{th}$ denote the global thumbnail features and $\mathbf{F}_p$ represent the local patch features. GAM establishes a bidirectional semantic alignment:

Global-to-Local: $\mathbf{f}_{th}$ serves as the Query to attend to $\mathbf{F}_p$, broadcasting global context to refine local feature extraction.

Local-to-Global: Local patches are aggregated to reconstruct and supplement the global representation.

By minimizing reconstruction error and fusing these views, GAM outputs contextually calibrated, aligned features $\mathbf{f}_{align}$. This ensures the model maintains focus on cellular atypia without losing sight of global patterns, such as glandular distribution.

Fuzzy-Guided Cross-Attention Module (FGCA) To synthesize information from the two visual streams, FGCA establishes a closed-loop interaction between the precise spatial features $\mathbf{f}_{align}$ and the abstract fuzzy features $\mathbf{f}_{fuzzy}$. We design a bidirectional cross-attention mechanism. In the first pathway, $\mathbf{f}_{align}$ serves as the Query to extract semantic guidance from $\mathbf{f}_{fuzzy}$ (Key/Value). In the second pathway, $\mathbf{f}_{fuzzy}$ queries $\mathbf{f}_{align}$ to anchor its uncertainty estimations onto concrete spatial structures. The outputs are fused via an adaptive gating network: $\mathbf{f}_{final} = \mathbf{g} \cdot \mathbf{f}'_{align} + (1 - \mathbf{g}) \cdot \mathbf{f}'_{fuzzy}$, where $\mathbf{g} = \sigma(\text{MLP}([\mathbf{f}'_{align}; \mathbf{f}'_{fuzzy}]))$. This gating mechanism dynamically balances the contributions of deterministic spatial evidence and fuzzy logic reasoning based on the input complexity.

2.3 Semantic Prior Path

This path aims to dynamically establish fine-grained semantic associations between local visual features of pathological images and medical prior knowledge in a zero-shot manner. The core idea is to treat image patches as routable information packets and softly align their semantic content with a predefined library of pathological text fragments.

Concept Bank & Soft Routing We construct a text library containing N pathological concepts (e.g., cribriform patterns, nuclear molding), which are encoded into embeddings $\mathbf{E}_{text}$ by a pre-trained VLM (Conch [16]). To simulate the semantic overlap inherent in pathology, we propose a Soft Routing Mechanism. Visual features $\mathbf{X}$ are projected into the text space, and their cosine similarities with $\mathbf{E}_{text}$ are calculated via temperature-scaled Softmax to generate the

routing weight vector $\mathbf{w}$:

$$w_i = \frac{\exp(\text{sim}(\text{Proj}(\mathbf{X}), \mathbf{e}_i)/\tau)}{\sum_{j=1}^{N} \exp(\text{sim}(\text{Proj}(\mathbf{X}), \mathbf{e}_j)/\tau)}. \tag{3}$$

Regularization & Alignment To enhance the interpretability of semantic matching and prevent the over-dispersion of attention weights, while ensuring that learned features possess semantic significance, we impose two constraints during training:

Sparsity Loss ($\mathcal{L}_{sparse}$): By utilizing negative entropy and L_1 regularization, we encourage the model to select a concentrated set of concepts rather than a uniform distribution.

Alignment Loss ($\mathcal{L}_{align}$): We explicitly minimize the distance between the projected visual features $\mathbf{z}_v = \text{Proj}(\mathbf{X})$ and the weighted sum of text embeddings $\mathbf{z}_t = \sum_i w_i \mathbf{e}_i$:$\mathcal{L}_{align} = 1 - \cos(\mathbf{z}_v, \mathbf{z}_t)$. This forces visual representations to align with human-interpretable medical concepts, thereby improving both performance and clinical trustworthiness.

3 Experiments

3.1 Datasets and Experimental Setup

We evaluated the medical image classification performance of DGFMIL on two publicly available pathological datasets: TCGA-CRC [24] and Camelyon17 [15]. These datasets encompass a diverse range of tissue types, varying numbers of categories, and various granular attributes. Our model is implemented in PyTorch and trained on an NVIDIA 4090 GPU. For the TCGA-CRC dataset, we employ an 8:1:1 split for the training, validation, and test sets, while the Camelyon17 dataset follows the official split protocols. In our architecture, the patch size is set to 256×256, and the thumbnails are downsampled to 512×512. We utilize the official pre-trained weights from Conch [16] for the encoder. The model is optimized using Cross-Entropy loss and Stochastic Gradient Descent (SGD), with an initial learning rate of 0.001 and a weight decay factor of 0.01. To evaluate the performance of DGFMIL, we adopt Accuracy (Acc), Area Under the Curve (AUC), Specificity (Spe), Recall, and F1-score (F1) as evaluation metrics. A five-fold cross-validation strategy is implemented, and all reported results consist of the mean and standard deviation across five independent runs.

3.2 Comparison Experiments

To demonstrate the superiority of our proposed method, we compare DGFMIL against several methods for similar tasks, including ABMIL [12], CoD-MIL [21], TransMIL [20], SGMF [22], CLAM [17], FMDNN [6], Conch [16]. As shown in Table 1 and Fig. 2, our model consistently outperforms existing baseline models on both the TCGA-CRC and Camelyon17 datasets. DGFMIL achieves significant advantages, particularly in cases with high morphological ambiguity.

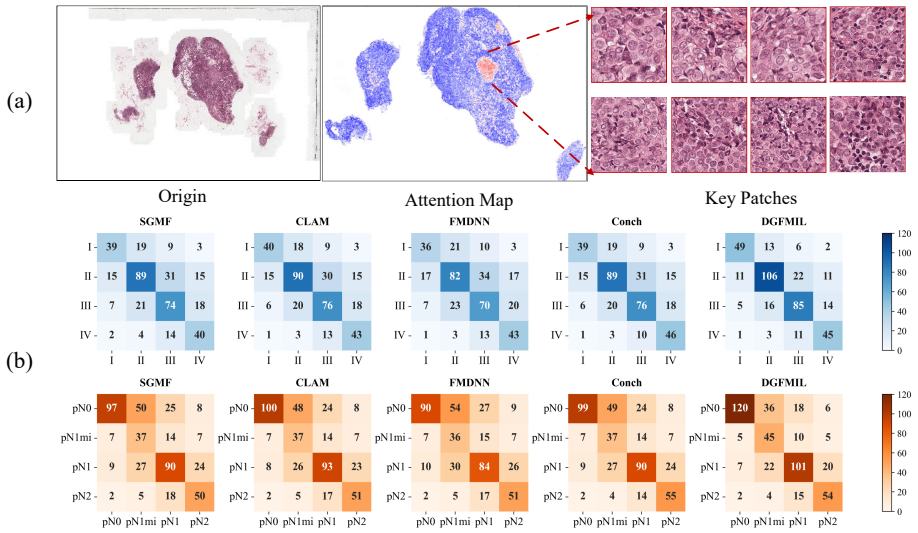

Fig. 2. (a) Visualization of a random sample;(b) Confusion matrices for some methods, the first row in blue shows results on TCGA-CRC dataset, the second row in orange shows results on Camelyon17 dataset.

Table 1. Comparison with several methods for similar tasks on cancer staging tasks (5-fold cross validation). The best results for each dataset are highlighted in bold.

Methods	Acc	AUC	Spe	Recall	F1
TCGA-CRC Dataset					
ABMIL	0.528±0.032	0.658±0.038	0.515±0.045	0.542±0.048	0.525±0.035
CoD-MIL	0.552±0.028	0.682±0.035	0.538±0.040	0.565±0.045	0.548±0.030
TransMIL	0.575±0.025	0.705±0.032	0.562±0.038	0.588±0.042	0.572±0.028
SGMF	0.598±0.022	0.728±0.029	0.585±0.035	0.612±0.038	0.595±0.025
CLAM	0.615±0.020	0.745±0.027	0.602±0.032	0.628±0.035	0.612±0.022
FMDNN	0.588±0.024	0.718±0.030	0.575±0.038	0.602±0.040	0.585±0.027
Conch	0.642±0.018	0.768±0.024	0.628±0.028	0.655±0.032	0.638±0.020
DGFMIL	**0.695±0.012**	**0.815±0.018**	**0.682±0.020**	**0.708±0.022**	**0.692±0.013**
Camelyon17 Dataset					
ABMIL	0.512±0.035	0.642±0.042	0.498±0.052	0.525±0.055	0.508±0.038
CoD-MIL	0.535±0.032	0.665±0.038	0.522±0.048	0.548±0.052	0.532±0.035
TransMIL	0.558±0.028	0.688±0.035	0.545±0.045	0.572±0.048	0.555±0.030
SGMF	0.582±0.025	0.712±0.032	0.568±0.040	0.595±0.045	0.578±0.028
CLAM	0.598±0.022	0.728±0.029	0.585±0.038	0.612±0.042	0.595±0.025
FMDNN	0.572±0.026	0.702±0.032	0.558±0.042	0.585±0.045	0.568±0.028
Conch	0.625±0.020	0.752±0.027	0.612±0.035	0.638±0.038	0.622±0.022
DGFMIL	**0.672±0.015**	**0.788±0.022**	**0.658±0.025**	**0.685±0.028**	**0.668±0.016**

This improvement stems from effectively modeling the inherent uncertainty of pathological boundaries—a characteristic that traditional clear-cut multi-class learning methods fail to capture. Regarding dataset differences, Camelyon17 is 2–3% lower than TCGA-CRC because lymph node metastasis staging is more challenging than overall staging tasks.

3.3 Ablation Study

We conduct comprehensive ablation studies to evaluate the contribution of each core component in our framework: the Membership Prior Attention Mechanism (MPAM), the Granularity Alignment Module (GAM), the Fuzzy-Guided Cross-Attention Module (FGCA), the routing soft alignment mechanism and the Interval Type-2 Fuzzy Sets (IT2FS).

We conduct comprehensive ablation studies to evaluate the contribution of each core component in our framework. As shown in Table 2, removing MPAM, GAM, FGCA, Text, and fuzzy module results in Acc drops of 11.3%, 10.0%, 10.7%, 8.7%, and 7.3%, respectively, demonstrating that all components contribute synergistically to the final performance. Notably, MPAM and GAM exhibit the most significant impacts, confirming that uncertainty-aware attention modulation and cross-scale alignment are indispensable for accurate cancer staging. Replacing IT2FS with traditional Type-1 fuzzy functions yields suboptimal results, validating the necessity of interval type-2 fuzzy logic for handling high-order uncertainties in histopathological image analysis.

Table 2. Ablation study results of DGFMIL on TCGA-CRC dataset (5-fold cross validation). The best results are highlighted in bold.

Methods	**Acc**	**AUC**	**Sp**	**Recall**	**F1**
w/o MPAM	0.582±0.028	0.712±0.031	0.568±0.035	0.595±0.042	0.578±0.029
w/o GAM	0.595±0.024	0.725±0.029	0.582±0.032	0.608±0.038	0.591±0.025
w/o FGCA	0.588±0.026	0.718±0.030	0.575±0.034	0.602±0.040	0.585±0.027
w/o Text	0.608±0.022	0.738±0.027	0.595±0.030	0.622±0.035	0.605±0.023
w/o fuzzy	0.622±0.020	0.752±0.025	0.608±0.028	0.635±0.032	0.618±0.021
Gaussian	0.642±0.018	0.768±0.024	0.628±0.026	0.655±0.030	0.638±0.019
Sigmoid	0.638±0.019	0.765±0.025	0.625±0.027	0.652±0.031	0.635±0.020
Trapezoidal	0.648±0.017	0.775±0.023	0.635±0.025	0.662±0.029	0.645±0.018
G+S+T	0.668±0.015	0.792±0.021	0.655±0.023	0.682±0.026	0.665±0.016
IT2FS(DGFMIL)	**0.695±0.012**	**0.815±0.018**	**0.682±0.020**	**0.708±0.022**	**0.692±0.013**

4 Conclusion

In this paper, we present DGFMil, a dual-granularity fuzzy MIL framework designed to handle the inherent ambiguity and multi-scale nature of WSIs-based disease staging. By integrating Interval Type-2 Fuzzy Sets and bidirectional

cross-granularity alignment, our model effectively captures uncertain boundary features while maintaining a global-to-local morphological context. Extensive evaluations on TCGA-CRC and Camelyon17 datasets demonstrate that DGFMIL significantly outperforms the compared methods in both classification accuracy and uncertainty quantification. Our ablation studies further confirm the necessity of each component in bridging the gap between low-level visual patterns and high-level pathological concepts. Future research will explore more robust uncertainty calibration techniques and extend this framework to diverse clinical tasks such as prognosis prediction.

Acknowledgments. This study was funded in part by the National Natural Science Foundation of China under Grant 62476190 and Grant 62376183, in part by the Shanxi Provincial Basic Research Program (Youth Project) under Grant 202403021212175.

Disclosure of Interests. The authors have no competing interests to declare that are relevant to the content of this article.

References

1. Beca, F., Polyak, K.: Intratumor heterogeneity in breast cancer. In: Novel biomarkers in the continuum of breast cancer, pp. 169–189. Springer (2016)
2. Belharbi, S., Rony, J., Dolz, J., Ayed, I.B., McCaffrey, L., Granger, E.: Deep interpretable classification and weakly-supervised segmentation of histology images via max-min uncertainty. IEEE Transactions on Medical Imaging **41**(3), 702–714 (2022)
3. Campanella, G., Hanna, M.G., Geneslaw, L., Miraflor, A., Werneck Krauss Silva, V., Busam, K.J., Brogi, E., Reuter, V.E., Klimstra, D.S., Fuchs, T.J.: Clinical-grade computational pathology using weakly supervised deep learning on whole slide images. Nature medicine **25**(8), 1301–1309 (2019)
4. Chen, R.J., Lu, M.Y., Wang, J., Williamson, D.F., Rodig, S.J., Lindeman, N.I., Mahmood, F.: Pathomic fusion: An integrated framework for fusing histopathology and genomic features for cancer diagnosis and prognosis. IEEE transactions on medical imaging **41**(4), 757–770 (2020)
5. Chen, R.J., Lu, M.Y., Williamson, D.F., Chen, T.Y., Lipkova, J., Noor, Z., Shaban, M., Shady, M., Williams, M., Joo, B., et al.: Pan-cancer integrative histology-genomic analysis via multimodal deep learning. Cancer cell **40**(8), 865–878 (2022)
6. Ding, W., Zhou, T., Huang, J., Jiang, S., Hou, T., Lin, C.T.: Fmdnn: A fuzzy-guided multigranular deep neural network for histopathological image classification. IEEE Transactions on Fuzzy Systems **32**(8), 4709–4723 (2024)
7. Elston, C.W., Ellis, I.O.: Pathological prognostic factors in breast cancer. i. the value of histological grade in breast cancer: experience from a large study with long-term follow-up. Histopathology **19**(5), 403–410 (1991)
8. Fisher, R., Pusztai, L., Swanton, C.: Cancer heterogeneity: implications for targeted therapeutics. British journal of cancer **108**(3), 479–485 (2013)
9. Fu, F., Zhang, X., Wang, Z., Xie, L., Fu, M., Peng, J., Wu, J., Wang, Z., Guan, T., He, Y., et al.: A pathology-attention multi-instance learning framework for multimodal classification of colorectal lesions. Frontiers in Pharmacology **16**, 1592950 (2025)

10. Guo, C., Pleiss, G., Sun, Y., Weinberger, K.Q.: On calibration of modern neural networks. In: International conference on machine learning. pp. 1321–1330. PMLR (2017)
11. Güven, Y., Köklü, A., Kumbasar, T.: Exploring zadeh's general type-2 fuzzy logic systems for uncertainty quantification. IEEE Transactions on Fuzzy Systems **33**(1), 314–324 (2025)
12. Ilse, M., Tomczak, J., Welling, M.: Attention-based deep multiple instance learning. In: International conference on machine learning. pp. 2127–2136. PMLR (2018)
13. Javed, S., Mahmood, A., Ganapathi, I.I., Dharejo, F.A., Werghi, N., Bennamoun, M.: Cplip: Zero-shot learning for histopathology with comprehensive vision-language alignment. In: Proceedings of the IEEE/CVF Conference on Computer Vision and Pattern Recognition. pp. 11450–11459 (2024)
14. Li, Q., Chen, Q.F., Liao, N.Q.: Graph neural network-based multi-scale whole slide image fusion for pt staging of muscle-invasive bladder cancer. Cancer Science **117**(3), 864–875 (2026)
15. Litjens, G., Bandi, P., Ehteshami Bejnordi, B., Geessink, O., Balkenhol, M., Bult, P., Halilovic, A., Hermsen, M., Van de Loo, R., Vogels, R., et al.: 1399 h&e-stained sentinel lymph node sections of breast cancer patients: the camelyon dataset. GigaScience **7**(6), giy065 (2018)
16. Lu, M.Y., Chen, B., Williamson, D.F., Chen, R.J., Liang, I., Ding, T., Jaume, G., Odintsov, I., Le, L.P., Gerber, G., et al.: A visual-language foundation model for computational pathology. Nature medicine **30**(3), 863–874 (2024)
17. Lu, M.Y., Williamson, D.F., Chen, T.Y., Chen, R.J., Barbieri, M., Mahmood, F.: Data-efficient and weakly supervised computational pathology on whole-slide images. Nature biomedical engineering **5**(6), 555–570 (2021)
18. McDonald, O.G., Li, X., Saunders, T., Tryggvadottir, R., Mentch, S.J., Warmoes, M.O., Word, A.E., Carrer, A., Salz, T.H., Natsume, S., et al.: Epigenomic reprogramming during pancreatic cancer progression links anabolic glucose metabolism to distant metastasis. Nature genetics **49**(3), 367–376 (2017)
19. Mendel, J.M., John, R.I., Liu, F.: Interval type-2 fuzzy logic systems made simple. IEEE transactions on fuzzy systems **14**(6), 808–821 (2006)
20. Shao, Z., Bian, H., Chen, Y., Wang, Y., Zhang, J., Ji, X., et al.: Transmil: Transformer based correlated multiple instance learning for whole slide image classification. Advances in Neural Information Processing Systems **34**, 2136–2147 (2021)
21. Shi, J., Li, C., Gong, T., Wang, C., Fu, H.: Cod-mil: chain-of-diagnosis prompting multiple instance learning for whole slide image classification. IEEE Transactions on Medical Imaging **44**(3), 1218–1229 (2024)
22. Shi, J., Tang, L., Li, Y., Zhang, X., Gao, Z., Zheng, Y., Wang, C., Gong, T., Li, C.: A structure-aware hierarchical graph-based multiple instance learning framework for pt staging in histopathological image. IEEE Transactions on Medical Imaging **42**(10), 3000–3011 (2023)
23. Sottoriva, A., Kang, H., Ma, Z., Graham, T.A., Salomon, M.P., Zhao, J., Marjoram, P., Siegmund, K., Press, M.F., Shibata, D., et al.: A big bang model of human colorectal tumor growth. Nature genetics **47**(3), 209–216 (2015)
24. The Cancer Genome Atlas Research Network, Weinstein, J.N., Collisson, E.A., Mills, G.B., Shaw, K.R.M., Ozenberger, B.A., Ellrott, K., Shmulevich, I., Sander, C., Stuart, J.M.: The cancer genome atlas pan-cancer analysis project. Nature Genetics **45**(10), 1113–1120 (2013)
25. Wang, X., Yang, S., Zhang, J., Wang, M., Zhang, J., Yang, W., Huang, J., Han, X.: Transformer-based unsupervised contrastive learning for histopathological image classification. Medical image analysis **81**, 102559 (2022)

26. Yao, J., Zhu, X., Huang, J.: Deep multi-instance learning for survival prediction from whole slide images. In: International Conference on Medical Image Computing and Computer-Assisted Intervention. pp. 496–504. Springer (2019)
27. Zhao, Z., Chen, K., Zhao, J.: Rpmil: Rethinking uncertainty-aware probabilistic multiple instance learning for whole slide pathology diagnosis. In: Proceedings of the 34th International Joint Conference on Artificial Intelligence, IJCAI 2025. pp. 2467–2475. International Joint Conferences on Artificial Intelligence (2025)